N89-12594

MULTIPLE INPUT/OUTPUT RANDOM VIBRATION CONTROL SYSTEM

James F. Unruh
Southwest Research Institute

ABSTRACT

A multi-input/output random vibration control algorithm was developed based on system identification concepts derived from random vibration spectral analysis theory. The unique features of the algorithm are: 1) the number of input excitors and the number of output control responses need not be identical, 2) the system inverse response matrix is obtained directly from the input/output spectral matrix, and 3) the system inverse response matrix is updated every control loop cycle to accommodate system amplitude nonlinearities. A laboratory demonstration case of two inputs with three outputs is presented to demonstrate the system capabilities.

INTRODUCTION

All products are subjected to vibration during their lives, either as a result of the manufacturing process, transportation or in-service environments. The capability of the product to withstand this vibration environment and to provide the desired reliability becomes a major design factor in high-technology applications where designs are constrained by severe environments, limited space envelopes, weight constraints and cost. These designs are often beyond the state-of-the-art in analysis procedures, and one is forced to simulate the product's environment to determine its reliability. To accurately estimate in-service reliability, it then becomes necessary to develop a simulation program which accurately reproduces field environments.

In the most general sense, a field vibration environment will consist of motion with six degrees of freedom. Presently available experimental hardware and control systems are limited in their capability to simulate this environment. Most tests are performed using uniaxial random excitation and repeating the excitation along three mutually perpendicular axes. The primary concern is that the mean-time-between-failure (MTBF) rates determined from uniaxial tests do not represent in-service MTBF rates. One problem is determining the duration of testing along each axis of a uniaxial test and the respective test level adjustments to account for physical coupling actually experienced in the field. Because of these uncertainties, the MTBF obtained from uniaxial test can only be considered an estimate of the in-service MTBF. For aerospace product development where product weight can have considerable influence on overall system performance, the need for reliable design evaluation is critical. A secondary consideration is the cost of three test setups to complete the simulation cycle in a uniaxial test.

To satisfy these shortcomings, it will be necessary to develop test facilities that simulate the field environments using multi-axis excitation. In the words of MIL-STD-810 (Ref. 1), the latest revision of the military's environmental test procedures, the test should be 'tailored' to measured field vibration. This will require multi-axis vibration systems with control of each axis and their interaction.

The objectives of the present study were to develop a multiple-input/output random vibration control algorithm based on system identification concepts derived from random vibration spectral analysis theory and to evaluate the usefulness of the algorithm via a laboratory-based demonstration.

A number of researchers have described in various detail the historical development of multi-axis/actuator control systems [Refs. 2-4]. Fisher at Lawrence Livermore Laboratory was one of the first to integrate a control theory and the required hardware to demonstrate system capabilities and limitations to perform multi-shaker vibration simulation [5]. The digital control system utilized a cross-coupling compensation matrix for signal control in the dc to 500 Hz frequency range. The major limitations of the system was the orthogonal axis excitation and the restriction that the number of response points must equal the number of excitation points.

Several multi-axis shaker systems are in present use; however, a number of them employ independent actuator control without cross-axis compensation. One exception is the facilities at Sandia National Laboratory [6-8] which has two-shaker random vibration control system with software capable of controlling up to four shakers. The control algorithm is based on determination of the inverse system frequency response matrix, which requires that the number of inputs and outputs must be identical. No capability exists for updating the system transfer function matrix directly during the control process, however, an incremental correction matrix is used to improve control.

There are several desired characteristics of a random vibration control algorithm that are believed to be important in simulating field vibration environments, they are: 1) Provide true stationary random excitation with near Gaussian amplitude distribution and signal crest factor (peak to r.m.s.) control; 2) Full control of cross-coupling between all output responses; 3) Number of input signals and number of output responses need not necessarily be the same; 4) Maintain loop equalization time to within a small fraction of total test time (say, less than 10%); and 5) Provide sufficient dynamic range and frequency bandwidth to meet simulation tolerances. Only when multi-axis testing becomes a reality can the degree of importance of each of these characteristics be determined.

In the sections to follow, a random vibration control algorithm is described that removes many of the limitations of existing algorithms, the software/hardware implementation of the algorithm is described, and an example of test results using the system are given to point out its capabilities and limitations. Several additional examples are given in Ref. 9.

CONTROL ALGORITHM FORMULATION

The development of the random vibration control algorithm views the simulation problem as one of system identification. The approach uses the spectral analysis techniques discussed in Ref. 10. For the purposes of discussion, consider the two-input/three-output simulation problem shown in Fig. 1. Physically, the "system" represents the dynamic response between voltage signals input into the vibration exciters, denoted as $x_1(t)$ and $x_2(t)$, and the response accelerations of an item attached to the exciters, denoted as $y_1(t)$, $y_2(t)$ and $y_3(t)$. The finite period (T) Fourier transform of the kth sample record is denoted as $X_i^k(f,T)$, $i = 1, 2$; and $Y_j^k(f,T)$, $j = 1, 2, 3$, respectively. The signal Fourier transforms are used to construct one-sided input/output cross-spectral densities as

$$G_{xy}^{ij}(f) = \lim_{T\to\infty} \frac{2}{T} E\,[X_i^k(f,T)^* \cdot Y_j^k(f,T)] \qquad (1)$$

with input auto-spectra,

$$G_{xx}^{ij}(f) = \lim_{T\to\infty} \frac{2}{T} E\,[X_i^k(f,T)^* \cdot X_j^k(f,T)] \qquad (2)$$

The output auto-spectra $G_{yy}^{ij}(f)$ is constructed in a similar way. The operator E is the mathematical expectation, and when averaged over N sample records of length T, the one-sided spectral density functions take the general form

$$G_{xy}^{ij}(f) = \frac{2}{NT} \sum_{k=1}^{N} E\,[X_i^k(f,T)^* \cdot Y_j^k(f,T)] \qquad (3)$$

where the * denotes the complex conjugate operator. The signals are assumed to be stationary random and, therefore, a finite number of samples, N, may be used to estimate the desired cross- and auto-spectra.

The system frequency response function, $[H_{yx}(f)]$, is defined by

$$\{Y(f)\} = [H_{yx}(f)]\{X(f)\} \qquad (4)$$

where the brackets { } denote the vector of response or input Fourier spectra. The inverse frequency response function, $[I_{xy}(f)]$, is defined as

$$\{X(f)\} = [I_{xy}(f)]\{Y(f)\} \qquad (5)$$

where the two system matrices are generally considered to be the inverse of each other. Such a concept is only valid when the number of input channels equals the number of output channels, which is not the general case considered in present development. To estimate $[I_{xy}(f)]$, we use the concept of mathematical expectation applied to Eq. 5 after post multiplying by the conjugate transpose of $\{Y(f)\}$, which, after some algebra, results in

$$[I_{xy}(f)] = [G_{xy}^*(f)][G_{yy}^*(f)]^{-1}. \qquad (6)$$

Thus, the system inverse response matrix is the product of the system input/output cross-spectral matrix and the inverse of the system output spectral matrix. It is important to note that when the system outputs are fully correlated, the output spectral matrix is rank deficient and the usual inverse is not defined. When this occurs one could drop control of one of the responses, combine two responses in an average or least squares way or define a pseudo inverse. The present algorithm employs a pseudo inverse as described by Greville [11]. The pseudo inverse routine produces the true inverse for rank sufficient matrices while producing unique inverses for rank deficient matrices. Due to extraneous noise at the output of most physical systems the pseudo inverse is often not necessary.

The relationship between the input auto-spectra and output auto-spectra is derived in a similar way as

$$[G_{xx}(f)] = [I_{xy}^*(f)][G_{yy}(f)][I_{xy}(f)]^T. \qquad (7)$$

Given a required output auto-spectra $[R_{yy}(f)]$, which is generally an envelope of multiple field measurements, the required input auto-spectra is defined by Eq. (7) as

$$[G_{xx}(f)] = [I^{*}_{xy}(f)][R_{yy}(f)][I_{xy}(f)]^{T}. \qquad (8)$$

The control problem becomes that of defining $\{X(f)\}$ such that the $[G_{xx}(f)]$ of Eq. (8) is realized. If the input signals were statistically independent random signals, there would be no output cross-coupling control other than that fixed by the physical exciters and test item arrangement. Thus, it becomes necessary to introduce cross-coupling control. This is accomplished by considering a coupling matrix $[A(f)]$ such that

$$\{X(f)\} = [A(f)]\{S(f)\}, \qquad (9)$$

where the $[A(f)]$ matrix is lower triangular (upper triangular elements are all zero) and the input $\{S(f)\}$ vectors are mutually independent white noise sources (unit r.m.s. amplitude with random phase). Upon post multiplication of Eq. (9) by the conjugate transpose of $\{X(f)\}$, and taking the mathematical expectation, there results an expression for the coupling elements in $[A(f)]$,

$$[A(f)][G_{ss}(f)][A^{*}(f)]^{T} = [G_{xx}(f)]. \qquad (10)$$

Since the input $\{S(f)\}$ vectors are mutually independent white noise, their spectral matrix $[G_{ss}(f)]$ is a unit diagonal matrix. A solution for the coupling elements in $[A]$ is given on page 262 of Ref. 10.

A flow chart is given in Fig. 2 which summarizes the major tasks of the control algorithm. To insure test item safety during control signal shaping, an incremental buildup to the full level drive has been introduced as denoted by the constant a and increment Δ a. As can be seen in Fig. 2, system amplitude nonlinearities are compensated via iteration by updating the system inverse response matrix $[I_{xy}(f)]$ every control loop. Maximum control is often achieved within two to three loop cycles as will be discussed in the results section.

Overall spectral error E_{yy} is generated for each output by computing the mean and standard deviation of the difference in logarithmic levels between the desired level R_{yy} and the measured level G_{yy} across the frequency spectrum. The maximum high and low values are also monitored. If control appears to be adequate, with less than a 2 to 3 dB mean variation, or improvement does not seem to be occurring, then individual spectrum plots are made to visually inspect the overall spectral matching achieved. The mean and standard deviation error estimates are useful for reducing the time consuming graphics data display during loop build up to the final drive level. Final judgment on acceptable drive levels are always made based on graphical inspection of the data.

SOFTWARE/HARDWARE IMPLEMENTATION

The hardware configuration used to implement the control algorithm was configured from two main stand alone processors. The drive signal generation and overall loop control is carried out via a 32-bit virtual memory laboratory computer. The laboratory computer generates the drive signals via a digital-to-

analog (DTA) interface and supplies control signals to a multi-channel fast Fourier transform (FFT) analyzer. The multi-channel FFT analyzer is capable of digitizing, Fourier transforming, and sample averaging up to 8 channels of data while maintaining time correlation. The input drive signals are sampled simultaneously with the output response signals so as to maintain correlation of all input and output signals. The various sample-averaged cross-spectral densities required by the control algorithm are transferred from the FFT analyzer to the laboratory computer via direct memory access (DMA). The transfer of one channel pair of auto- and cross-complex spectra (400 line) requires approximately 50 milliseconds. A two-input/four-output system requires transfer of 14 channel pairs of information, thus requiring approximately 0.7 seconds. The spectra transfer generally requires far less time than the sample averaging time required for a confident data sample when considering random error.

Drive Signal Generation

As previously stated, the approach taken to generate the required input drive signals is to consider the shaker inputs to be a combination of statistically independent random, stationary Gaussian signals $\{S_i\}$, i=1,2,3 ...M. In which case, the required drive signals $\{X_j\}$, j=1,2,3 ...N can be related to the ideal signals $\{S\}$ via a lower triangular coupling matrix [A]. The initial drive signals are generated first in terms of their spectral content; namely, unit amplitudes exist from the lowest frequency, f_L, to the highest frequency, f_H, of interest for output control. Using a uniformly distributed random number generator, the phase of each spectral component is generated with random variation from component to component. To be consistent with the FFT analyzer, a maximum of 400 spectral lines exist between zero frequency and the analyzer cutoff frequency. The analyzer cutoff frequencies, f_C, are predefined and selected such that $f_H \leq f_C$. As such, the Fourier spectrum of the drive signals initially consist of unit amplitude random phase components in the analysis range f_L to f_H. Finite length time histories of the initial signals are then obtained via the inverse Fourier transform of each independent signal.

In order to capture a number of independent random sample averages of the system response, sequences of the time histories must be continuously generated. If the same time series for a particular channel is repeatedly generated, the output wave form becomes pseudo-random and not acceptable for environmental simulation. To form acceptable drive signals, sequences of the same signal were randomly delayed by approximately 25 percent of the signal period and summed for output. It was found that if the signal time delay were fixed and not randomized, the resulting signals showed marked periodic components with unacceptable coherence between "independent" drive signals, as is shown in Fig. 3. However, when introducing the randomized time delays, acceptable signals such as shown in Fig. 4 resulted. It was found that the random phase relationship between the original independent drive signals $\{S\}$ could only be maintained when introducing the coupling matrix in the following partitioned form (as for a two-input system):

$$\left[\begin{array}{c|c} X_{11} & 0 \\ \hline X_{21} & X_{22} \end{array}\right] = \left[\begin{array}{c|c} A_{11} & 0 \\ \hline A_{21} & A_{22} \end{array}\right] \left[\begin{array}{c|c} S_1 & 0 \\ \hline 0 & S_2 \end{array}\right] \qquad (11)$$

Time histories are generated for the X_{11}, X_{21} and X_{22} signals individually where X_{11} and X_{21} maintain identical random phase shifts and random time lags as specified by the original generation of S_1, and X_{22} that of S_2. The desired time history drive signals corresponding to the specified coupling (the A matrix) are then

$$x_1(t) = x_{11}(t)$$

and

$$x_2(t) = x_{21}(t) + x_{22}(t). \qquad (12)$$

Additional important characteristics of the drive signals are that they be stationary and that the signal crest factor can be controlled. Stationarity is measured by the variation in signal mean and r.m.s. level as time progresses. For the present algorithm, the zero mean and r.m.s. variation are less than 1 percent. Control over peak-to-r.m.s. level is accomplished by introducing signal peak folding. All data points exceeding the desired peak value are folded back into the signal, not clipped at the peak value. Thus, signal peaks when folded become local valleys which tend to raise the signal r.m.s. level. Crest factor control in the range from 2.0 to 4.5 is readily accomplished.

Output Spectra Specification

In order to accommodate various levels of output control specification which presently exist for equipment under qualification and provide a means to evaluate the importance of all elements in a specification, the following specifications for the R_{yy} spectral matrix were developed.

1) Full R_{yy} Specification: where auto-spectra are specified by spectrum frequency and magnitude break point pairs and cross-spectra are specified by spectrum frequency, magnitude, and phase break point values.

2) Auto-Spectra and Coherence Specification: where auto-spectra are specified by spectrum frequency and magnitude break point pairs and cross-spectra are specified by frequency and coherence break point pairs. Herein, the cross-spectra magnitudes are generated from the definition of spectral coherence,

$$\gamma^2_{ij} = \frac{|G_{ij}|^2}{G_{ii}G_{jj}} \qquad (13)$$

and the phase of R_{yy} is taken as that of the measured G_{yy}.

3) Auto-Spectra Only: where auto-spectra are specified by frequency and magnitude break point pairs. The cross-spectra magnitude and phase are generated from the measured G_{yy} in proportion to the magnitude of the specified R_{yy} via:

$$R_{ij} = \frac{(R_{ii} \cdot R_{jj})^{\frac{1}{2}}}{(G_{ii} \cdot G_{jj})^{\frac{1}{2}}} \cdot G_{ij} \qquad (14)$$

For existing test specifications such as MIL-STD-810C/D, only the output auto-spectra may be known. If field measurements were made without specification of cross-spectra, one may be much better off to accept the cross-axis coupling of the

test setup rather than attempting to invoke a physically unrealizable specification for which control would be impossible or which may drastically alter the service life of the test item.

TYPICAL RESULTS

Several types of exciters, exciter arrangements, and test item configurations were used to evaluate the proposed control algorithm and its limitations as reported in Ref. 9. The algorithm evaluation process will, of course, continue as the system is employed for equipment qualification purposes, and the author is confident that much is to be learned as opportunities arise for its use. The following example illustrates the general capabilities of the control algorithm.

Multi-Resonant Beam

In order to study the control of sharp structural resonances a small cantilever beam was driven using two small voice coil shakers. Three accelerometers were used to record the beam response. The two-input/three-output system is schematically shown in Fig. 5.

The cantilever beam exhibited damping of less than 0.3% critical, which is uncharacteristic of built-up structures in which damping levels of 2 to 5% are more representative. Thus, the low damped beam provides a harsh test of the control algorithm to control resonances. The initial drive signals to the exciters are shown in Fig. 6 as being independent random signals in the frequency range from 5 to 250 Hz. The initial beam response to the drive signals and the desired output magnitude specifications are shown in Fig. 7. Due to the sharp resonances in the beam, exhibiting distinct phase between outputs, only the cross-axis coherence was specified since the excitors were of marginal power and, thus, not likely powerful enough to change system phasing. The coherence between output channels 1 and 2 was set at 0.50, as was that between channels 2 and 3. The coherence between channels 1 and 3 was set to 0.20. Control after three loop iterations resulted in the output spectra shown in Fig. 8. As can be seen, the primary beam resonance was well-controlled, as was the second beam resonance at outputs 2 and 3. Since output 1 was at an anti-node of the second beam resonance, sensitivity to the second mode was high at that location as is shown in Fig. 8a. The second beam resonance occurs around 90 Hz and with a critical damping ratio of 0.003, its half-power point bandwidth would be approximately 0.54 Hz. Thus, with a control bandwith of 0.625 Hz (250 Hz/400 lines), reasonably good control of the mode was realized. Control of the cross-spectra was reasonably good, however, not as good as the auto-spectra shown in Fig. 8.

Aircraft External Store Vibration Simulation

The aircraft external store used to evaluate a two-input/four-output control configuration is shown in Fig. 9. The external store is a dummy test item with an overall length of 193.3 cm (76.12 inches). Major bulkheads are at Missile Stations (MS) 30.38, 55.06 and 66.125. The bulkheads provide for exciter attachment and free-free missile suspension via elastic bungy cords (2 Hz vertical). The test item is fitted with add-on damping material to raise modal damping values to 0.02 minimum. A dynamic modal analysis of the test item in the frequency range from 10 to 500 Hz revealed an abundance of normal mode resonances as shown in Table 1. It was felt that this multi-modal structure would provide a good evaluation of the proposed control algorithm.

Input excitation to the test item was provided by two electrodynamic modal shakers attached at MS 30.38 and MS 66.125. The shakers were aligned normal to the missile longitudinal axis and 45 degrees to the vertical (see Fig. 9). The acceleration response control points are located at MS 55.06 and MS 30.38 with one vertical and one horizontal transducer at each location. Response channels 1 and 4 are the horizontal responses and channels 2 and 3 the vertical responses. Field data were not available for the test item and, therefore, the control specification was a flat response in the frequency range from 20 to 500 Hz on each output with magnitude 10^{-4} g^2/Hz. The bandwidth of resolution was set at 1.25 Hz which should provide marginal resolution to control a 2% damped 100 Hz mode (half power point bandwidth of 4.0 Hz).

The output response specification for channels 1 and 3, along with the recorded responses after the initial broadband excitation and after three control loop cycles, are shown in Fig. 10. As can be seen by the data given in Fig. 10a, channel 1 response was initially dominated by the fuselage first and second horizontal modes; nevertheless, the control algorithm performed reasonably well. Similar trends were seen in the other responses as well as is shown in Fig. 10b for the channel 3 response. Close examination of the hay-stack response in the area of 460 Hz in channel 3 response shows the incompatibility of the control specification relative to the location of the excitors and response accelerometers. In this case, it was impossible to drive response 4 (not shown) in the horizontal direction to the desired level while maintaining vertical response to within limits in the frequency region of the third fuselage vertical bending mode at 462.5 Hz. For the most part, the control algorithm performed well, except at these incompatible areas. It is expected that measured field data would not reflect these incompatibilities if the exciters were placed at the store-to-aircraft attachment points and field data were recorded at the specified output locations.

Throughout the evaluations discussed above, 20 sample averages were used to obtain the results shown. In many cases, 5-10 averages would have been adequate during signal development. A higher number of averages, on the order of 200, are appropriate for random data analyses of the final drive signals to establish statistical confidence [10]. Control loop time is highly dependent on the frequency range of interest and the graphical display of results. Twenty sample averages at a maximum frequency of 62.5 Hz requires 128 seconds; while for an analysis out to 2000 Hz, the sample average time is only 4 seconds. Thus, in the former case, 10 seconds for control analysis time is insignificant while in the latter case it is measurable. In either case, the time to record graphical data to a hardcopy device is significant. Such intermediate output records can, of course, be avoided after developing confidence in the algorithm.

CONCLUSIONS AND RECOMMENDATIONS

Based on the limited experience gained with the control algorithm thus far, the following conclusions and observations are made:

1) It appears that the control algorithm, as implemented, will allow different numbers of input and output channels. This feature can be useful in various practical test situations, including assurance of uniform excitation for a test item.

2) The algorithm updates the system inverse response matrix every control loop cycle which accommodates system amplitude nonlinearities and allows compensation for system degradation during life time simulation.

3) Full control of cross-coupling between all output responses can be invoked with the present algorithm. However, it appears that the extent to which control is achieved is highly dependent on the physical arrangement of the exciters.

4) Analysis bandwidth is an important parameter in controlling test item resonances. The 400-line analysis used in the present system appears to be marginal, with 800 to 1000-line analysis being preferred.

5) The dynamic range of the present system is set by the FFT analyzer, that being the 12-bit analog-to-digital converters. It is recommended that 16-bit resolution be used to insure sufficient dynamic range especially for random signal control where crest factors of 3 to 4.5 are required.

SYMBOLS

Values are given in both SI and U.S. Customary Units. The measurements and calculations were made in U.S. Customary Units.

f_L, f_C, f_H	low, center, and high frequency, Hz
t	time, sec.
X_i	input voltages of the i^{th} channel, volts
Y_j	output accelerations of the j^{th} channel, g
$A(t)$	lower triangular coupling matrix
E	mathematical expectation operator
E_{yy}	Overall output spectral error, g^2/Hz
$G_{xy}^{ij}(f)$	one-sided input/output cross-spectral density, volt-g/Hz
$G_{xx}^{ij}(f)$	one-sided input auto-spectral density, $volts^2$/Hz
$G_{yy}^{ij}(f)$	one-sided output auto-spectral density, g^2/Hz
$H_{yx}(f)$	system frequency response function, g/volt
$I_{xy}(f)$	system inverse frequency response function, volt/g
N	number of sample records
$S(t)$	independent random white noise sources, volt
T	finite period of time, sec.
$X_i^k(f,T)$	k^{th} sample record of finite period Fournier Transform of $X_i(t)$, g-sec
$Y_j^k(f,T)$	k^{th} sample record of finite period Fournier Transform of $Y_j(t)$, g-sec
γ_{ij}	spectral coherence (Eq. 13)
$*$	complex conjugate operator

REFERENCES

1. MIL-STD-810D, "Environmental Test Methods and Engineering Guidelines", July 19, 1983.

2. Everett, W. D., and Helfrich, T. M. "Triaxial Vibration System," 55th Shock and Vibration Bulletin, Part 2, June 1985, pp. 1-15.

3. Fisher, K. K., "Theoretical and Practical Aspects of Multiple-Actuator Shaker Control," 43rd Shock and Vibration Bulletin, Part 3, June 1973, pp. 153-174.

4. Smith, S., Stroud, R. C., Hamma, G. A., and Johnson, L#ntrol System for Testing a Single Test Item with Multiple Inputs," SAE Paper 821482, 1982.

5. Fisher, D. K., and Posehn, M. R., "Digital Control for a Multiple-Actuator Shaker," 47th Shock and Vibration Bulletin, Part 3, September 1977, pp. 77-96.

6. Tebbs, J. D., and Hunter, N. F., Jr., "Digital Control of Random Vibration Tests Using a Sigma V Computer," Proceedings, Institute of Environmental Sciences, 1974, pp. 36-43.

7. Smallwood, D. O., "A Random Vibration Control System for Testing a Single Test Item with Multiple Inputs," SAE Paper 821482, 1982.

8. Smallwood, D. O., "Random Vibration Testing of a Single Test Item with a Multiple Input Control System," Proceedings, Institute of Environmental Sciences, 1982, pp. 42-49.

9. Unruh, J. F., "Multiple Input/Output Random Vibration Control System," Southwest Research Institute Internal Research Report No. 06-9465, April 1988.

10. Bendat, J. S., and Piersol, A. G., Engineering Applications of Correlation and Spectral Analysis, John Wiley & Sons, 1980.

11. Greville, T. N. E., "Some Applications of the Pseudo-Inverse of a Matrix," SIAM Review, II, pp. 15-32, 1960.

Table 1. External Store Natural Frequencies

Mode No.	Frequency (Hz)		Mode Description
1	15.0	1st	Symmetric Wing Vertical Bending
2	52.5		Symmetric Wing Torsion
3	57.5		Coupled Tail/Wing Horizontal
4	97.5	1st	Fuselage Vertical Bending
5	102.5	1st	Fuselage Vertical Bending
6	107.5	1st	Fuselage Horizontal Bending
7	120.0	2nd	Symmetric Wing Vertical Bending
8	202.5	2nd	Fuselage Horizontal Bending
9	227.5	2nd	Fuselage Vertical Beding
10	390.0		Wing Panel Mode
11	410.0		Wing Panel Mode
12	435.0	2nd	Fuselage Horizontal Bending
13	462.5	3rd	Fuselage Vertical Bending + 2nd Wing

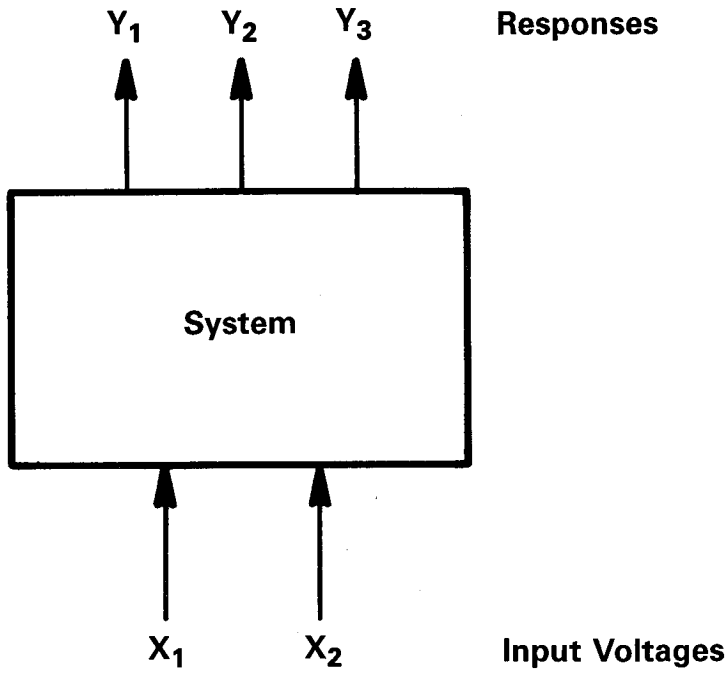

Figure 1. Two-Input/Three-Output System

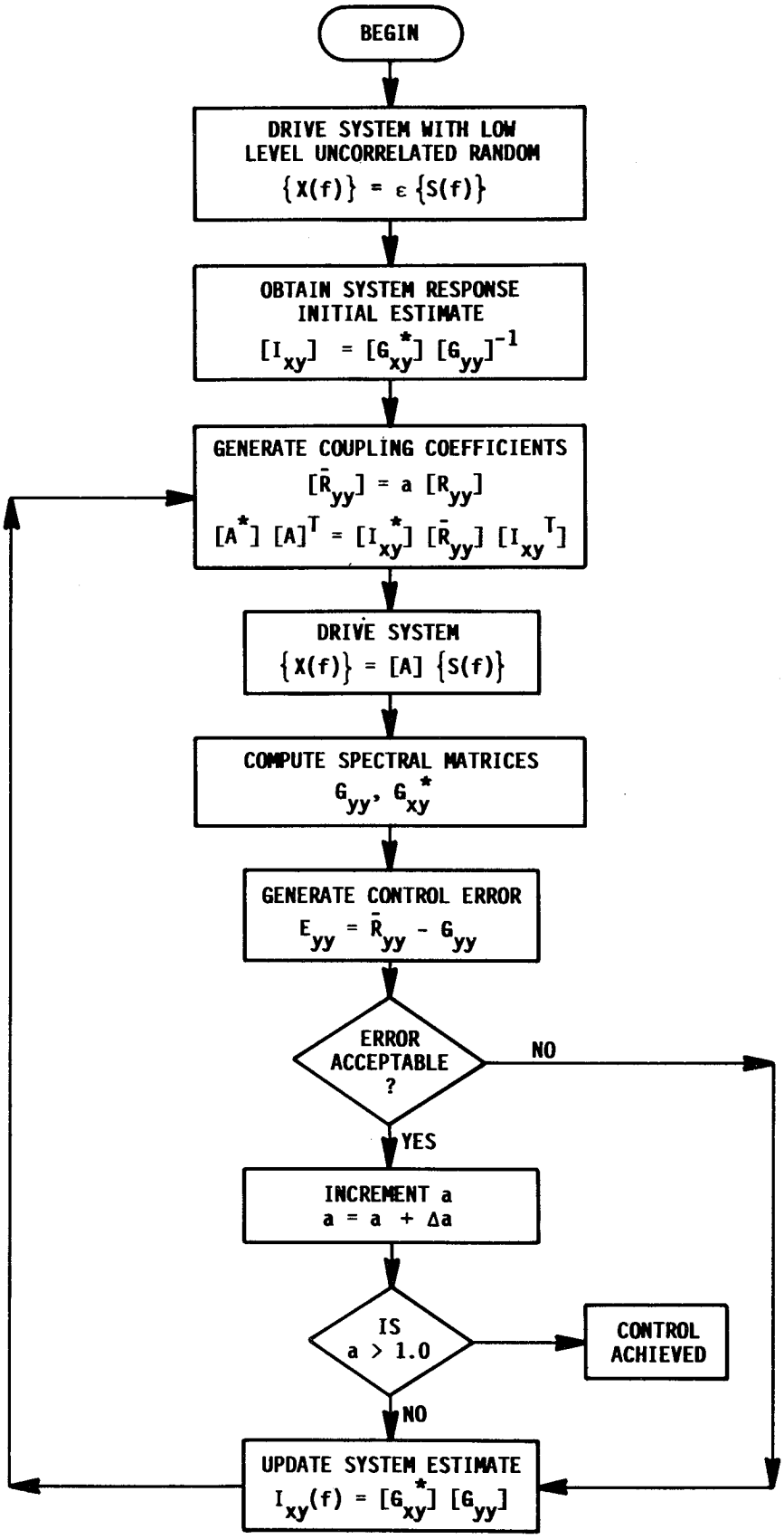

Figure 2. Control Algorithm Flow Chart

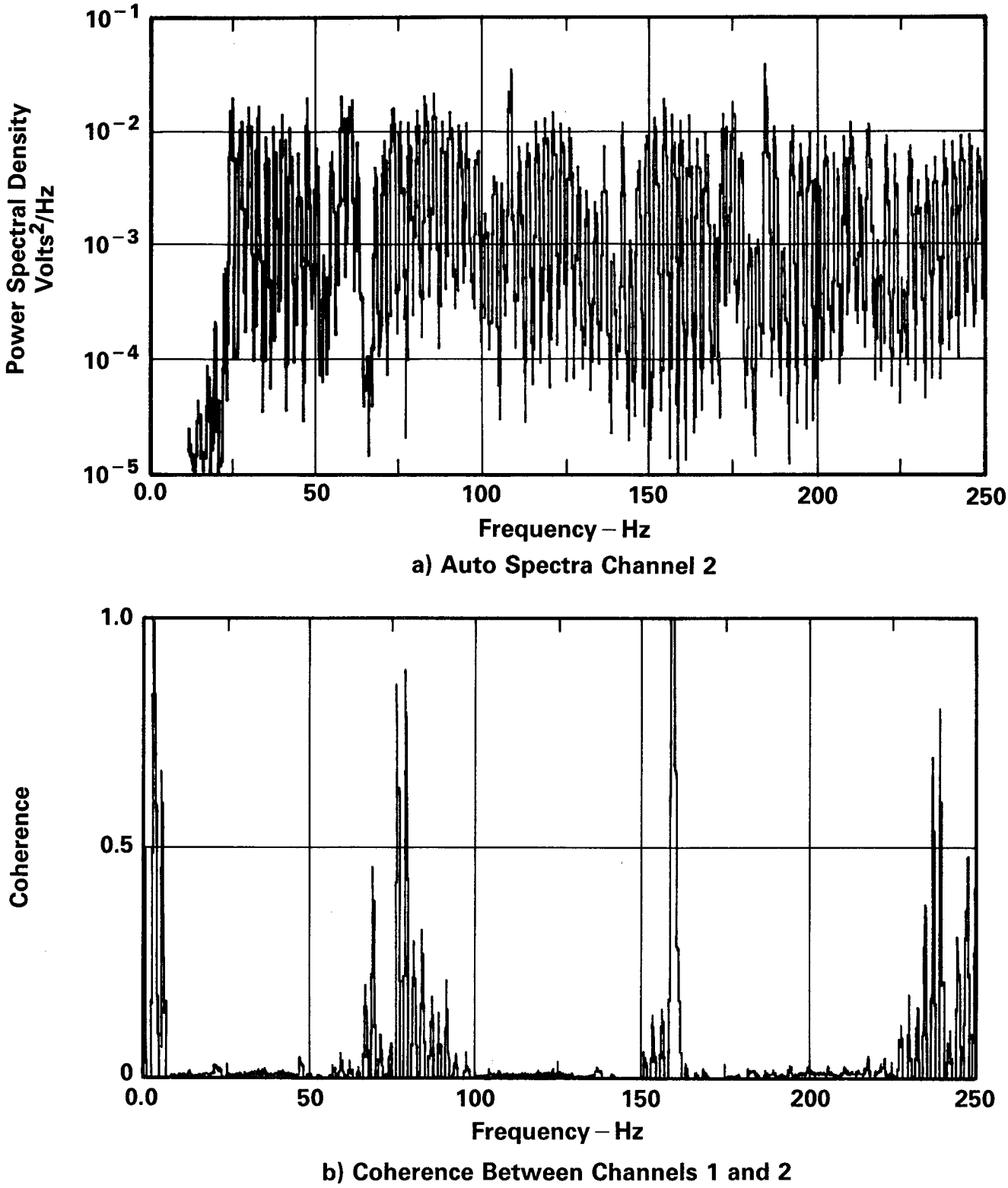

Figure 3. Typical Spectral Averaged Drive Signals, Fixed Time Delay During Time Sequence Generation

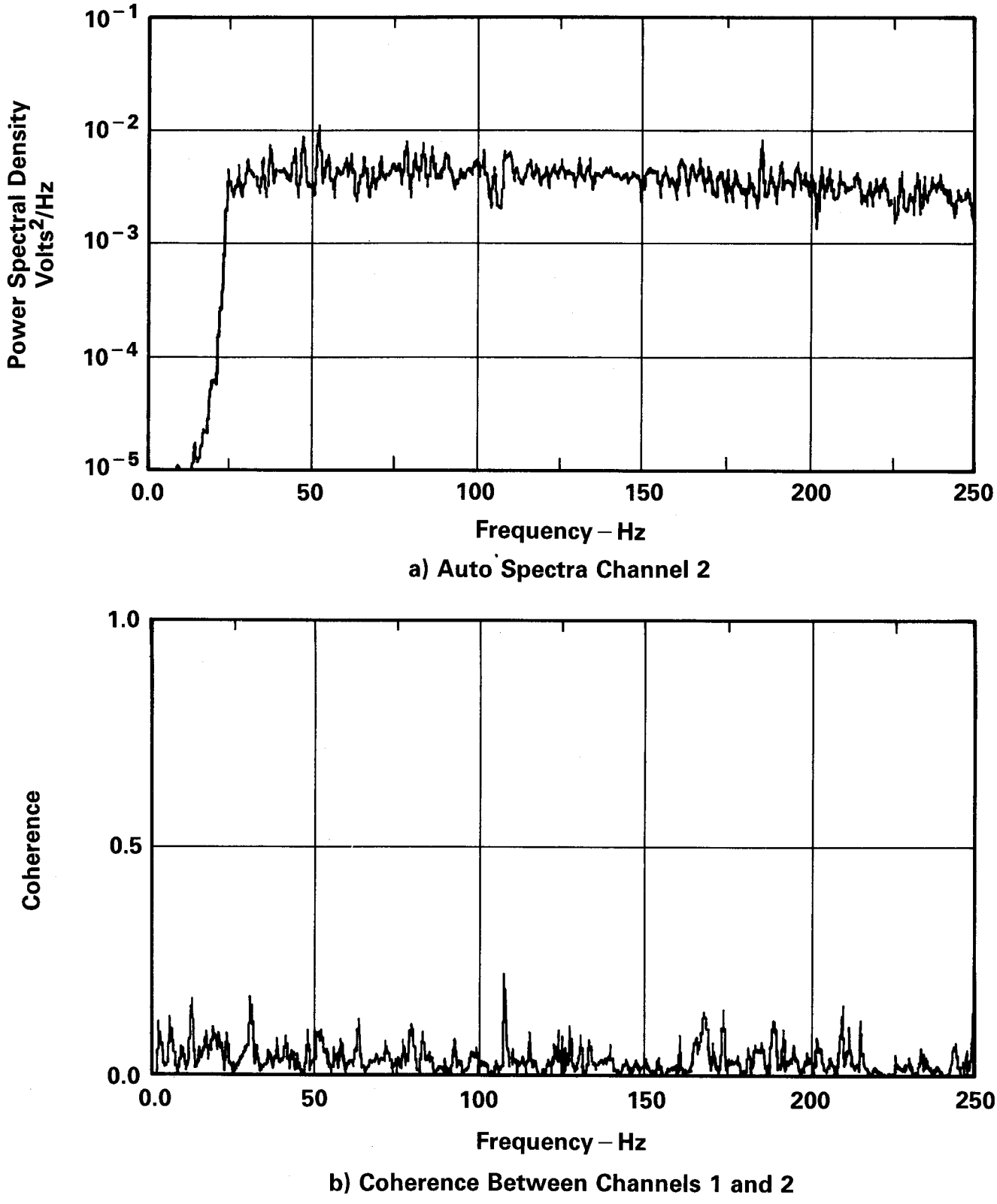

Figure 4. Typical Spectral Averaged Drive Signals, Random Time Delay During Time Sequence Generation

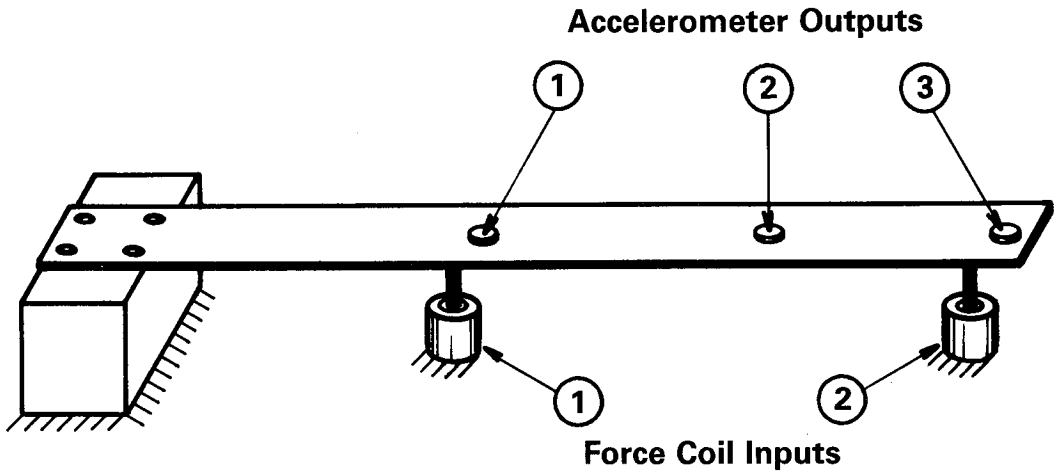

Figure 5. Schematic of the Two-Input/Three-Output System

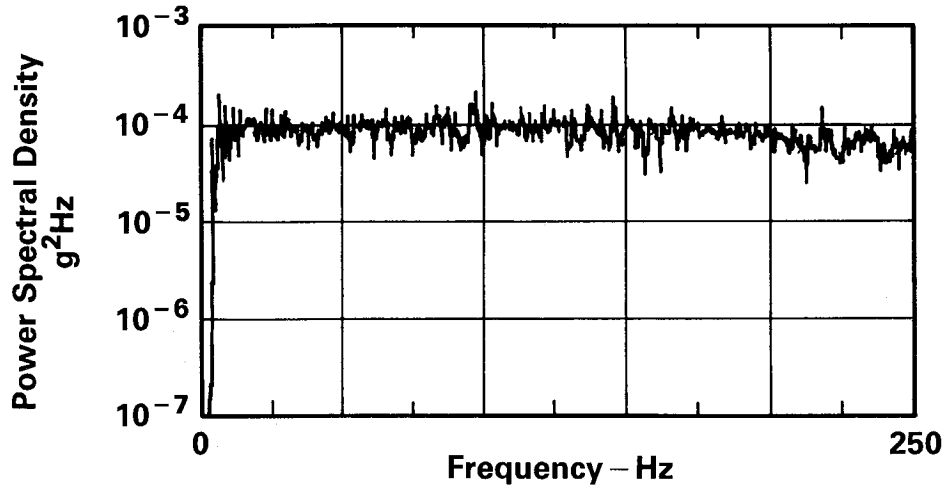

a) PSD – Channel 1 or Channel 2

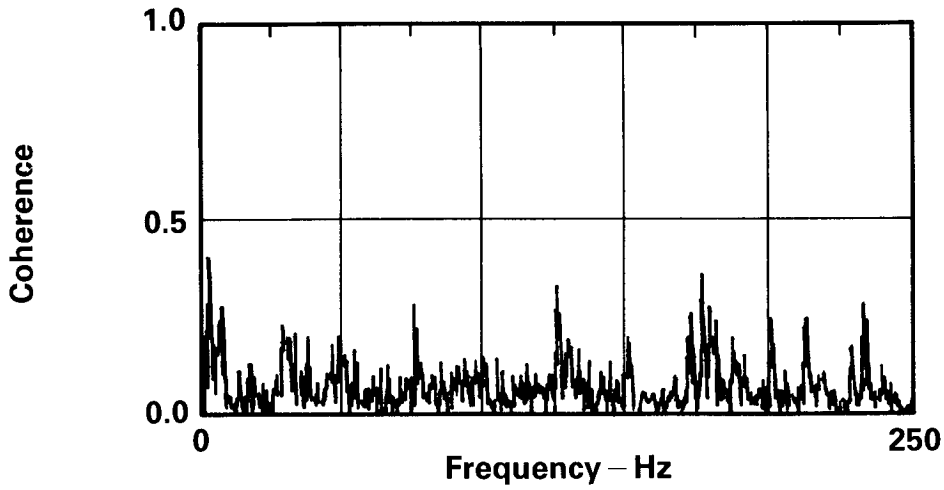

b) Coherence Channel 2 to Channel 1

Figure 6. Initial Drive Signals

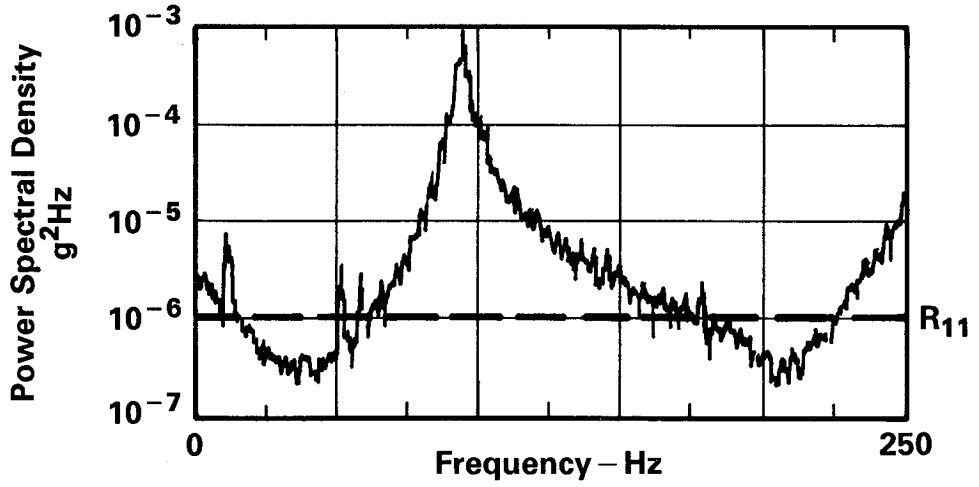

a) Output PSD Channel 1

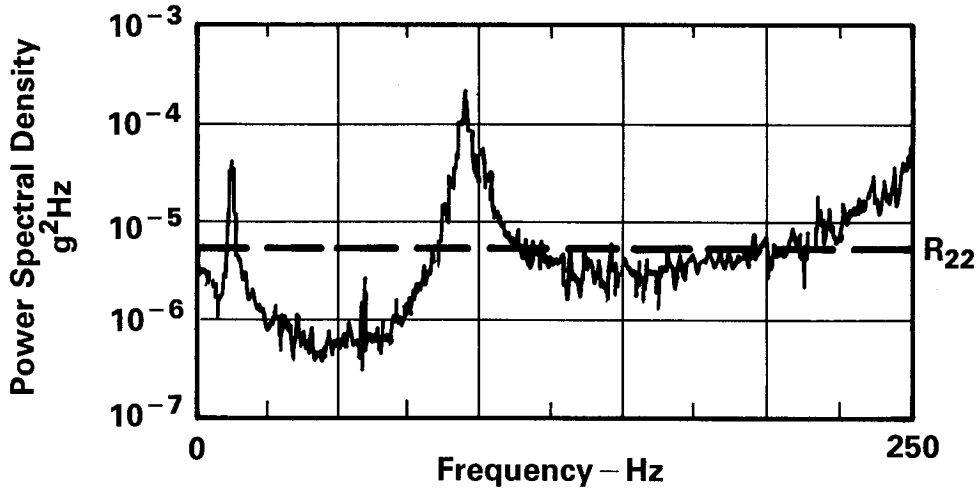

b) Output PSD Channel 2

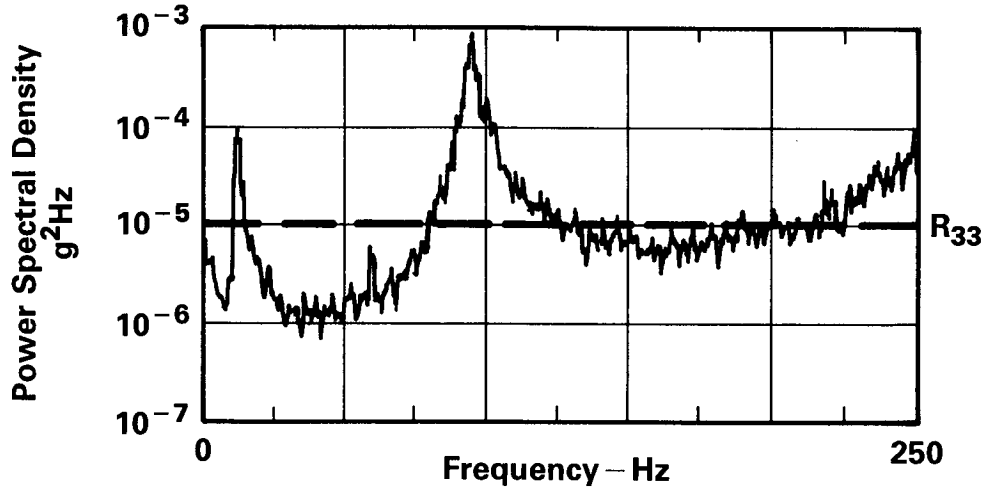

c) Output PSD Channel 3

Figure 7. Initial Beam Response

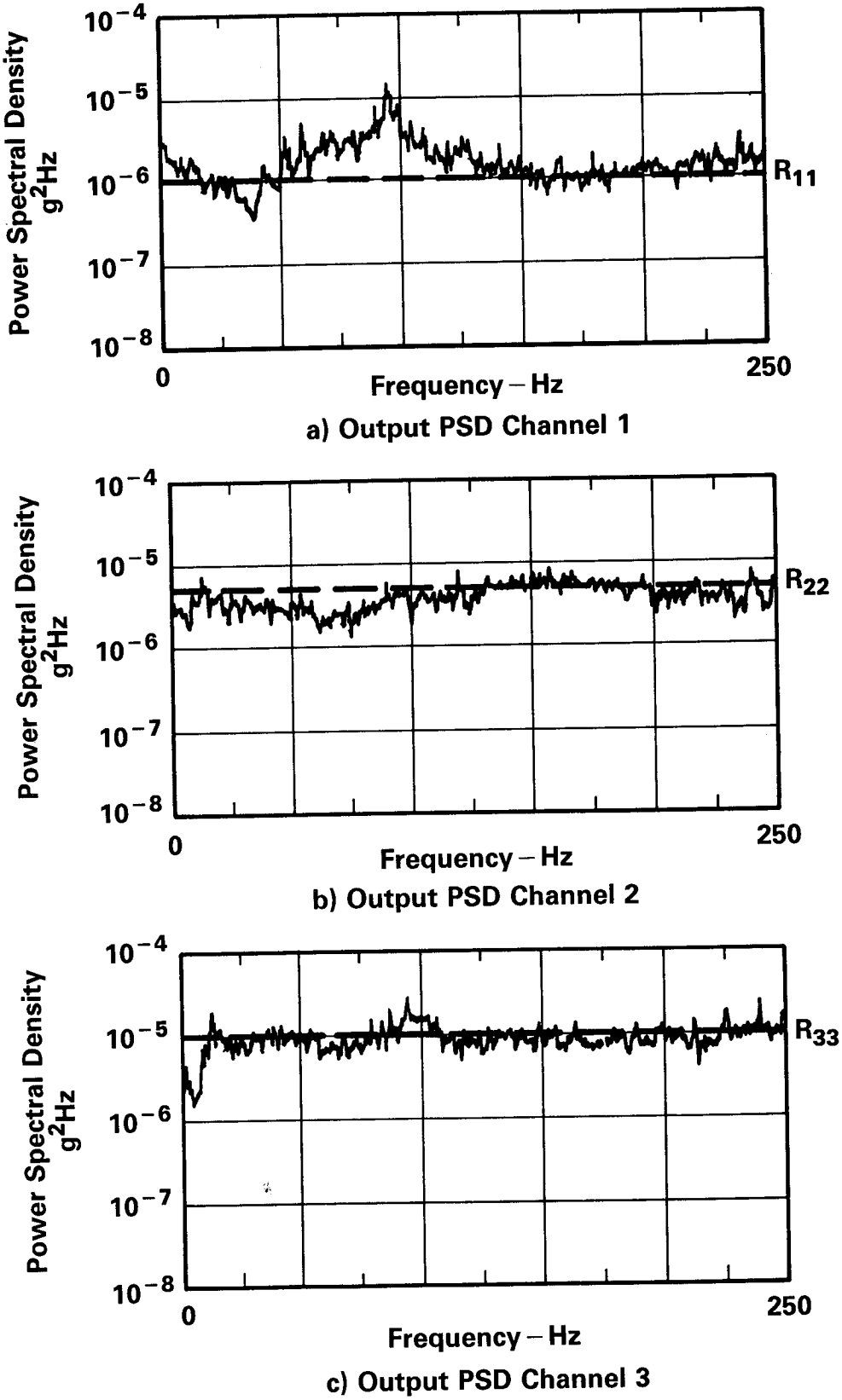

Figure 8. Beam Response After Three Iterations

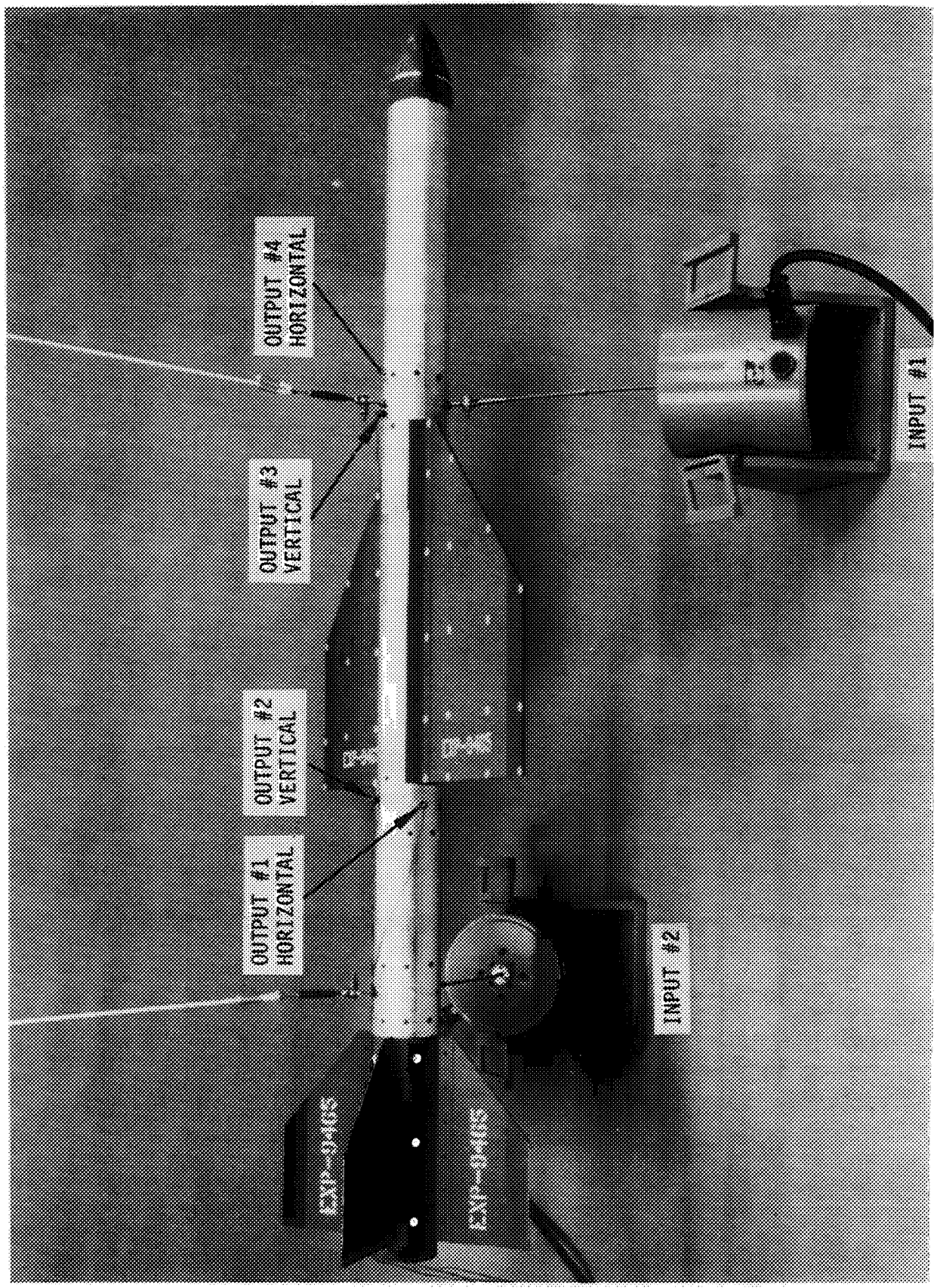

Figure 9. Aircraft External Store Test Configuration

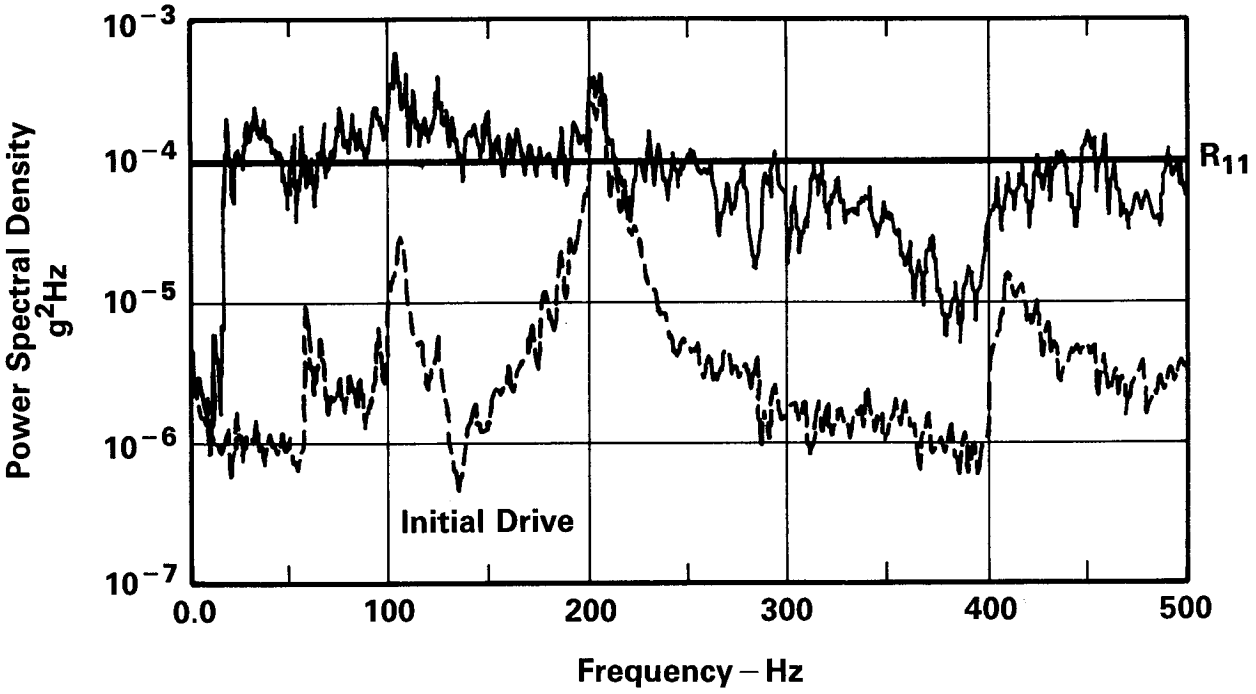

a) Output PSD Channel 1

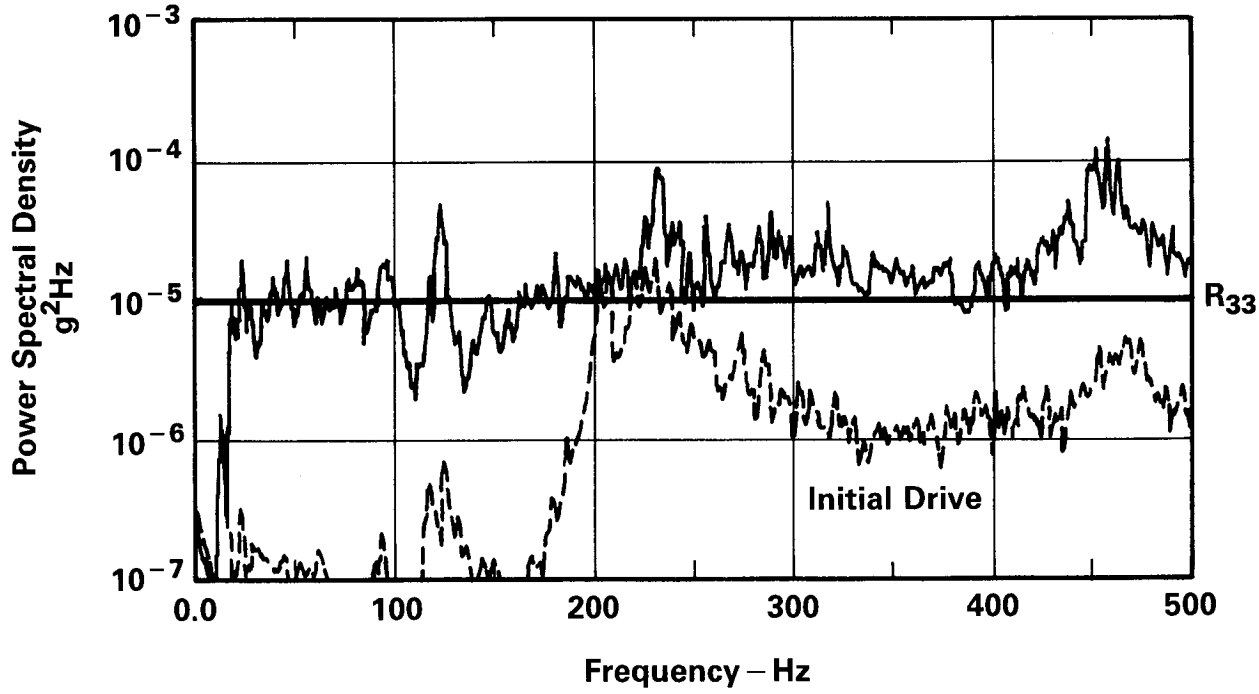

b) Output PSD Channel 2

Figure 10. External Store Response